Molecular Therapy
Nucleic Acids
Original Article

Circular RNA Expression Profiling and the Potential Role of hsa_circ_0089172 in Hashimoto's Thyroiditis via Sponging miR125a-3p

Si Xiong,[1,4] Huiyong Peng,[2,4] Xiangmei Ding,[1] Xuehua Wang,[1] Li Wang,[1] Chenguang Wu,[1] Shengjun Wang,[2] Huaxi Xu,[3] and Yingzhao Liu[1]

[1]Department of Endocrinology, The Affiliated People's Hospital, Jiangsu University, Zhenjiang 212002, China; [2]Department of Laboratory Medicine, The Affiliated People's Hospital, Jiangsu University, Zhenjiang 212002, China; [3]Institute of Laboratory Medicine, Jiangsu Key Laboratory of Laboratory Medicine, Jiangsu University School of Medicine, Zhenjiang 212013, China

Circular RNA (circRNA) is a novel subclass of noncoding-RNA molecules that participate in development and progression of a variety of human diseases via sponging microRNAs (miRNAs), but the role of circRNAs in Hashimoto's thyroiditis (HT) has not been defined. In this study, peripheral blood samples from five patients with HT and five healthy volunteers were investigated by Illumina HiSeq Sequencer. A total of 627 differentially expressed circRNAs including 370 upregulated and 257 downregulated ones were identified in HT patients. Four upregulated circRNAs indicated the same rising tendency toward sequencing results. The expression of hsa_circ_0089172 was upregulated and correlated positively with the serum level of the thyroid peroxidase antibody. Two perfectly matched binding sites of miR-125a-3p were found in hsa_circ_0089172 sequences with bioinformatics tools. The expression of miR-125a-3p was decreased in the HT patients and correlated inversely with an elevated level of hsa_circ_0089172. Moreover, knockdown of hsa_circ_0089172 resulted in an increase of the expression of miR-125a-3p *in vitro*. Receiver operating characteristic (ROC) curve analysis suggested that hsa_circ_0089172 had significant value in HT diagnosis. Taken together, these results demonstrate that hsa_circ_0089172 as a potential diagnostic biomarker of HT and may play a crucial role in the pathogenesis of HT via sponging miR-125a-3p.

INTRODUCTION

Hashimoto's thyroiditis (HT), also called chronic lymphocytic thyroiditis, is a clinical, organ-specific autoimmune disease characterized by the pathological appearance of the thyroid gland.[1] It was initially described by Dr. Hakaru Hashimoto in 1912, but was only rarely reported until the early 1950s.[2,3] The main pathological features include lymphocytic infiltration in germinal centers, diffuse enlargement of the thyroid gland, destruction and atrophy of thyrocytes, and interstitial fibrosis. The serological feature is persistent positivity of thyroid autoantibodies including thyroglobulin antibody (TGAb) and thyroid peroxidase antibody (TPOAb).[4,5] The pathogenesis of HT depends on many elements, including genetic predisposition, environmental implication, and immunological factors. Some HT patients suffer from transient hyperthyroidism during the disease process, but the majority ultimately develop hypothyroidism.[6,7] HT is considered a common autoimmune thyroid disease, as well as the cause of the hypothyroidism. However, our understanding of the pathogenesis of HT is still very limited.[8,9]

Circular RNAs (circRNAs) have recently been appreciated as a rediscovered species of noncoding RNAs (ncRNAs) that emerge during RNA maturation through a process called back splicing.[10–12] They are cyclic in structure, are derived from exons and introns of gene fragments, and have considerable abundance, high conservation, and relative stability in the eukaryotic transcriptome. Certain kinds of circRNAs have been found to regulate gene expression at the transcriptional or post-transcriptional levels through sponging microRNAs (miRNAs) or binding to proteins of the target gene.[13–15] Previous studies have reported that circRNAs are involved in the regulation of the pathogenesis of various diseases, such as cancer, cardiovascular diseases, and autoimmune diseases.[16–19] In vascular diseases, circ_Lrp6 plays an important role in the regulation of vascular smooth muscle cells (VSMCs) migration, proliferation, and differentiation, by inhibiting miR-145 expression.[16] The roles of circRNAs in cancer initiation and progression have also been described. An example is circ-CTNNB1, which is derived from the CTNNB1 intron and has been identified as a mediator of β-catenin signaling that promotes cancer progression through bridging DEAD-box polypeptide 3 (DDX3) to interact with transcription factor Yin Yang 1 (YY1), resulting in transactivation of YY1.[17] In addition, hsa_circ_0045272 has been found to regulate apoptosis and interleukin-2 secretion negatively in systemic lupus erythematosus (SLE),[18] and circRNA_104871 significantly elevates in

Received 17 January 2019; accepted 5 May 2019;
https://doi.org/10.1016/j.omtn.2019.05.004.

[4]These authors contributed equally to this work.

Correspondence: Yingzhao Liu, MD, PhD, Department of Endocrinology, The Affiliated People's Hospital, Jiangsu University, Dianli Road 8, Zhenjiang 212002, China.
E-mail: zjliuyingzhao@126.com

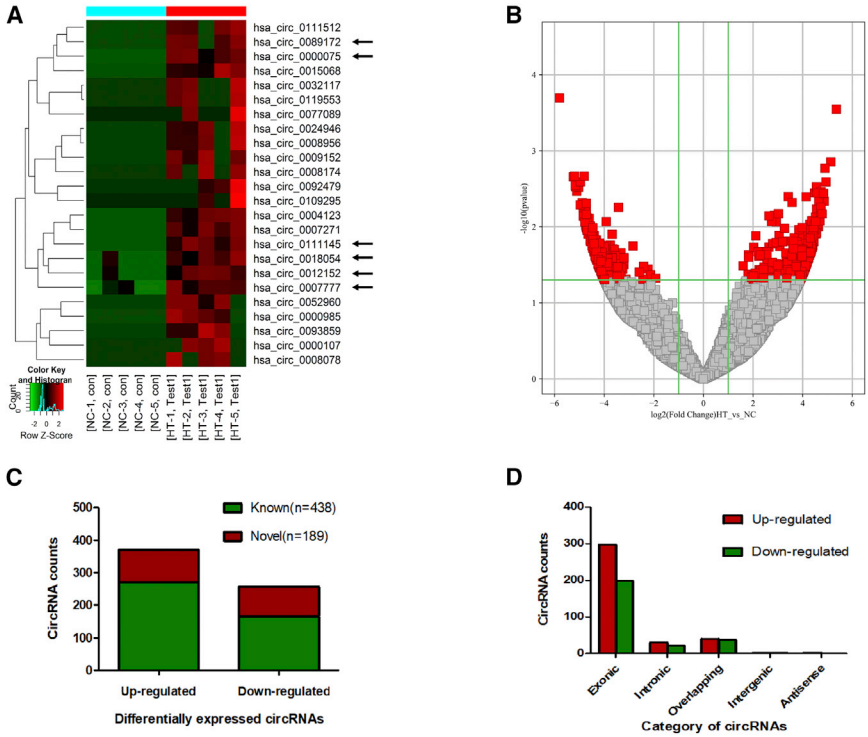

Figure 1. Expression Profiling of circRNAs in PBMCs from Patients with Hashimoto's Thyroiditis and Normal Controls

(A) In the clustered heatmap identified by next-generation sequencing, each column represents peripheral blood mononuclear cells (PBMCs) from a patient or a healthy volunteer, each line represents a circRNA. The red lines are upregulated circRNAs, and the green ones are downregulated circRNAs. Six upregulated circRNAs which were verified by real-time qPCR were marked. (B) Differentially expressed circRNAs between Hashimoto's thyroiditis (HT) and normal controls (NC) are displayed by volcano plots. Vertical green lines indicate 2-fold ($\log_2$ scaled) up or down changes, and the horizontal green line indicates a p value of 0.05 ($-\log_{10}$ scaled). Red squares represent circRNAs with statistically significant differences in expression. (C) Of the 627 circRNAs with significant different expression, 370 markedly upregulated circRNAs and 257 notably downregulated circRNAs were identified. Among them, there were 189 novel circRNAs (red) and 438 circRNAs (green) which had been identified before. (D) The number of upregulated (red) and downregulated (green) circRNAs according to their categories of formation mode.

rheumatoid arthritis (RA).[19] These findings suggest that circRNAs play a significant role in the pathogenesis of human diseases and may serve as potential biomarkers for diseases diagnosis. However, little is known about the expression profiles and functions of circRNAs in HT. Our previous study showed that miR-125a-3p significantly decreases in patients with HT and is involved in the pathogenesis of HT via targeting IL-23R.[20] However, the relationship between circRNAs and miR-125a-3p in HT is not yet known.

In this study, next-generation sequencing (NGS) was applied to identify differentially expressed circRNAs between HT and health controls. We aimed to identify circRNA profiling in peripheral blood mononuclear cells (PBMCs) from patients with HT and to explore the roles of circRNAs in the pathogenesis of HT. We found that hsa_circ_0089172 expression was markedly increased and correlated inversely with reduced levels of miR-125a-3p in HT patients. Two perfectly matched binding sequences were found between hsa_circ_0089172 and miR-125a-3p. Knockdown of hsa_circ_0089172 led to upregulation of miR-125a-3p and downregulation of IL-23R mRNA *in vitro*. Moreover, receiver operating characteristic (ROC) curve analysis suggested that hsa_circ_0089172 has significant value in the diagnosis of HT.

RESULTS

RNA Quality Control

The Nano-Drop ND-1000 was used for RNA quality control. Denatured agarose gel electrophoresis was applied to test RNA integrity. The optic density OD A260/A280 ratio was set close to 2.0 for pure RNA (ratios between 1.8 and 2.1 were accredited), and the standard OD A260/A230 ratio was set at >1.8 for spectrophotometer readings. As for the agarose gels, rRNA bands of 28S and 18S had to be pointed and of high intensity, whereas bands of low-molecular-weight RNAs such as 5S rRNA or tRNA were had to be diffuse and smaller. A high-molecular-weight dispersion or a band migrating above the 28S rRNA band was evidence of DNA contamination. All quality criteria established by the manufacturer were achieved.

Expression Profiling of circRNAs in Patients with HT

The differentiated circRNAs between the HT and normal control (NC) groups with statistical criteria were determined through fold change and p value (fold change $\geq$ 2.0; p value $\leq$ 0.05). Finally, 627 significantly differentially expressed circRNAs were identified. In contrast to the NC group, a total of 370 circRNAs were markedly upregulated, and 257 were significantly downregulated in the HT group, as shown by a cluster heatmap (Figure 1A) and a volcano plot (Figure 1B).

Among the 627 differentially expressed circRNAs, 189, including 98 upregulated ones and 91 downregulated ones, were verified as novel circRNAs; 438 circRNAs, including 272 upregulated and 166 downregulated ones, had been identified beforehand and listed in the circRNA database (circBase; http://www.circbase.org) or articles (Figure 1C). The 627 identified circRNAs were divided into five different categories on the basis of the way they were produced. Exonic circRNAs consisting of the protein-encoding exons accounted for 78.95% (495/627), intronic circRNAs from intron lariats comprised 8.13% (53/627), sense overlapping circRNAs that originated from exon and other sequence circRNAs comprised 12.28% (77/627), intergenic circRNAs composed of unannotated sequences of the gene

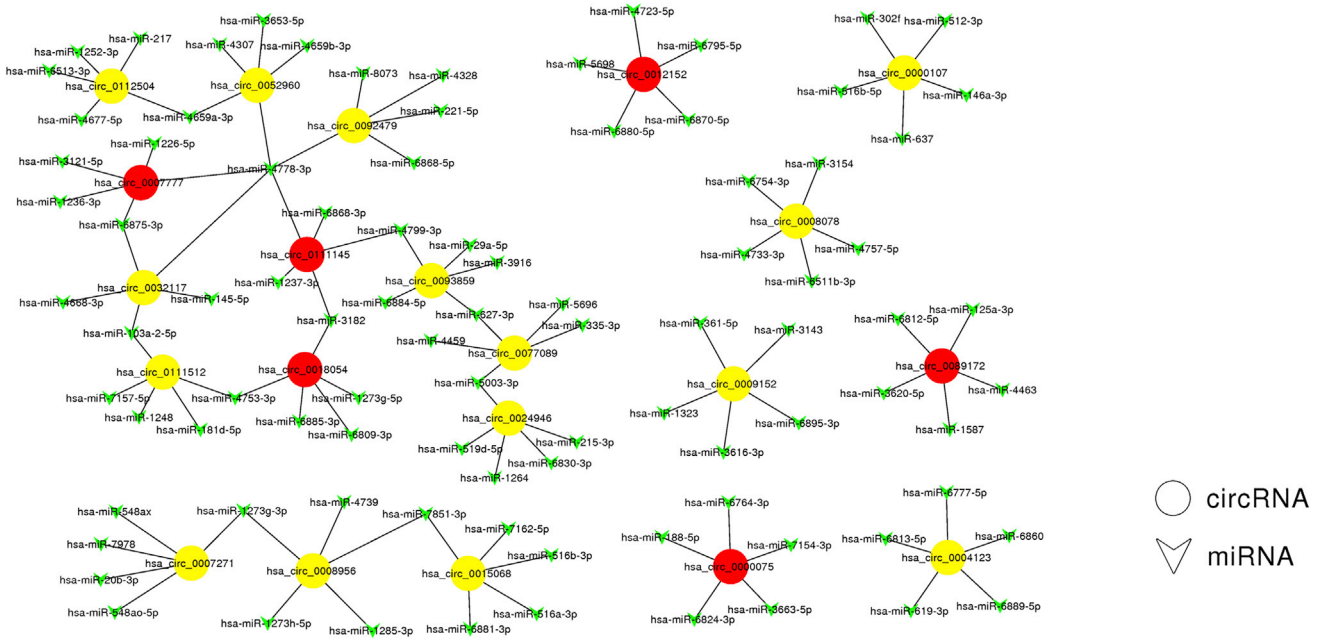

Figure 2. The Interaction Network between Differentially Expressed circRNAs and miRNAs in Hashimoto's Thyroiditis

Twenty-one upregulated circRNAs that were in circBase, including 15 circRNAs that ranked in the top 20 upregulated circRNAs (yellow) and 6 circRNAs that were selected for validation (red), are displayed in a network diagram. The top 5 miRNAs regulated by each circRNA are shown (green). Circles indicate circRNAs and arrows represent miRNAs.

and antisense circRNAs originating from antisense regions equally comprised 0.32% (2/627) (Figure 1D).

Interaction between Differentially Expressed circRNAs and miRNAs in the HT Group

miRNAs matched with circRNAs were explored to evaluate the potential functions of differentially expressed circRNAs in HT. A total of 459,846 miRNAs binding to their corresponding circRNAs were identified. According to the degree of enrichment, the top five miRNA response elements (MREs) were selected and listed. TargetScan and miRanda were used to conduct the analysis. Twenty-one circRNAs that were deposited in circBase, including 15 circRNAs that ranked in the top 20 upregulated circRNAs and 6 circRNAs that were selected for validation (Table S1), accompanied by the top 5 correlated miRNAs, are displayed in the form of a network graph produced by Cytoscape software. The graph shows that circRNAs interacted with miRNAs in a many-to-many way (Figure 2).

Function of Differentially Expressed circRNAs in HT

Gene Ontology (GO) and Kyoto Encyclopedia of Genes and Genomes (KEGG) analysis of source genes were used to explore functions of differentially expressed circRNAs. GO enrichment analysis of the source gene was made up of biological processes (BPs), cellular components (CCs), and molecular functions (MFs). Because the majority of the differentially expressed circRNAs were upregulated in the HT group compared with the NC group (Figure 1A), we placed emphasis on GO analysis of the 370 noteworthy upregulated circRNAs. The degree of enrichment was taken as the measurement standard, and the top 10 GO terms were identified. "Nucleocytoplasmic transporter activity," "pre-mRNA binding," and "FAD binding" were the top three in MFs (Figure 3A); "regulation of RNA export from nucleus," "Golgi to endosome transport," and "negative regulation of DNA-dependent DNA replication" were the top three BPs (Figure 3B); and "dendrite cytoplasm," "clathrin coat of coated pit," and "nuclear pore outer ring" were the top three CCs (Figure 3C).

The KEGG analysis made it possible to identify BFs of differentially expressed circRNAs through pinpointing pathways relevant to their source genes. The molecular datasets of genomics, transcriptomics, proteomics, and metabolomics were mapped to the KEGG pathways, to illuminate the biological functions of these molecules. Finally, 73 pathways connected with functions of 370 upregulated circRNAs in the HT group were defined by the KEGG analysis (data not shown). Moreover, the mitogen-activated protein kinase (MAPK), hypoxia inducible factor-1 (HIF-1), and chemokine signaling pathways were involved in regulating the expression of NF-κB among the 73 pathways (Figure 4), and NF-κB has been shown to be a pivotal factor in the pathogenesis of HT.

Verification of Selected circRNAs

PBMCs from 30 HT patients and 30 healthy volunteers were used for verification by real-time qPCR. Because markedly upregulated circRNAs made up approximately 60% of all the differentially expressed circRNAs and in order to make the information accessible for further research, we focused our attention on upregulated circRNAs with certain circBase IDs and singled out six of these circRNAs, with

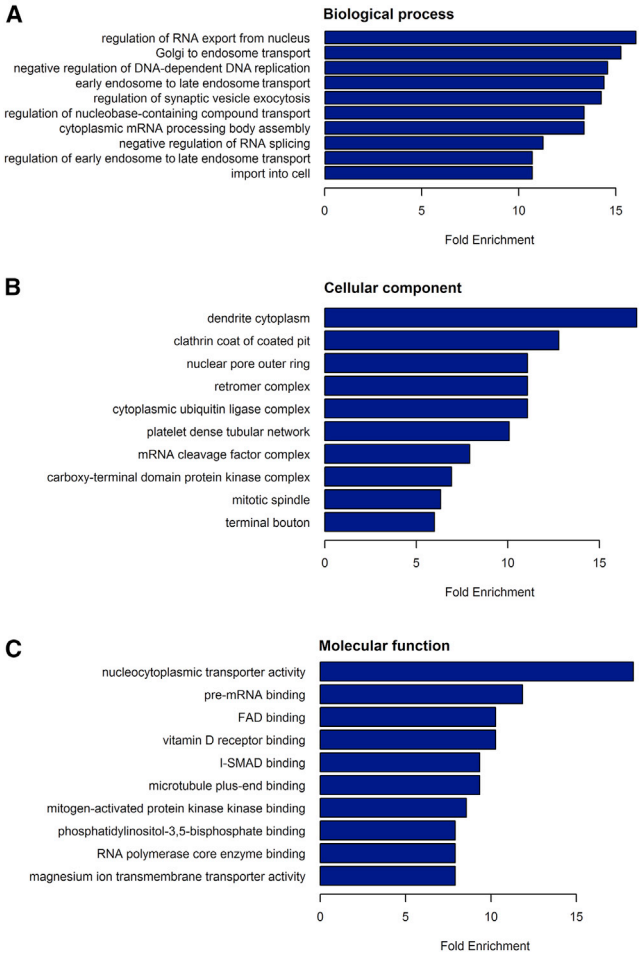

Figure 3. Function Predictions of Upregulated circRNAs in Hashimoto's Thyroiditis

Gene oncology (GO) enrichment analysis was made up of (A) biological processes, (B) cellular components, and (C) molecular functions. The top 10 predicted functions of the source gene regulated by 370 upregulated circRNAs in PBMCs from patients with HT were explored by GO analysis. Fold enrichment indicated the regulated extent of the predicted functions by upregulated circRNAs in Hashimoto's thyroiditis (HT) patients compared with normal controls (NC).

copy numbers that were significantly higher and were evenly distributed in each sample of the HT group, for validation of NGS. Among the selected six circRNAs, the expression levels of hsa_circ_0089172 ($p = 0.02$), hsa_circ_0007777($p = 0.01$), hsa_circ_0012152($p = 0.01$), and hsa_circ_0000075 ($p < 0.01$) in the HT group were apparently higher than in the NC group, whereas there was no statistically significant difference in the expression of hsa_circ_0018054 and hsa_circ_0111145 between the HT and NC groups (Figure 5).

ROC Curve Analysis of Confirmed circRNAs in PBMCs

ROC curve analysis was conducted to evaluate the potential diagnostic value of significantly and differentially expressed circRNAs. ROC curves of confirmed circRNAs showed that levels of hsa_circ_0089172, hsa_circ_0000075, and hsa_circ_0012152 could separate the patients with HT from the NCs. The highest area under the curve (AUC) was found for hsa_circ_0000075 (AUC 0.715, 95% CI 0.581–0.849, $p = 0.006$), followed by hsa_circ_0012152 (AUC 0.702, 95% CI 0.559–0.846, $p = 0.010$) and hsa_circ_0089172 (AUC 0.673, 95% CI 0.530–0.816, $p = 0.026$). Thus, it appeared that hsa_circ_0000075 ($p < 0.01$) may be more valuable than the other two circRNAs as a biomarker for RA diagnosis (Figure 6).

Correlation between hsa_circ_0089172 and Clinical Disease Activities

The relationship between the expression of six validated circRNAs and thyroid autoimmune antibodies which could reflect the severity of the disease was analyzed. The expression of hsa_circ_0089172 correlated positively with that of TPOAb in plasma, whereas there was no significant association between the expression of hsa_circ_0089172 and TGAb in patients with HT (Figure 7).

Correlation between hsa_circ_0089172 and miR-125a-3p

It was reported that the expression of miR-125a-3p was decreased in patients with HT. In addition, miR-125a-3p could be involved in the pathogenesis of HT through regulating expression of IL-23R, and miR-125a-3p was predicted to be a target of hsa_circ_0089172, according to our sequencing results (Figure 8D). Therefore, we investigated the interaction of hsa_circ_0089172 with miR-125a-3p. It was found that expression of miR-125a-3p significantly decreased in the HT group compared with the NC group, which was consistent with our previous study (Figure 8A), and expression of miR-125-3p showed negative correlation with that of hsa_circ_0089172 (Figure 8B). Subsequently, the binding sequence between hsa_circ_0089172 and miR-125a-3p was explored by Target-Scan and miRanda analysis. Two perfectly matched sequences of hsa_circ_0089172 binding with miR-125a-3p were identified (Figure 8C).

Influence of hsa_circ_0089172 on Expression of miR-125a-3p and IL-23R mRNA

To determine whether hsa_circ_0089172 affects the expression of miR-125a-3p and IL-23R mRNA, purified PBMCs from healthy volunteers were transfected with hsa_circ_0089172 small interfering RNA (siRNA) and a negative control. Manipulation of hsa_circ_0089172-specific siRNA resulted in the reduction of the transcript level of hsa_circ_0089172 compared with that of the negative control (Figure 8E). Downregulated expression of hsa_circ_0089172 with siRNA resulted in an increase in the transcript level of miR-125a-3p and reduction of transcript level of IL-23R mRNA compared with that of the negative control (Figures 8F and 8G). Together, these results indicate that hsa_circ_0089172 regulates the expression of miR-125a-3p in human PBMCs.

DISCUSSION

HT is an autoimmune disease that is characterized by long-term positivity for thyroid autoimmune antibodies, including TPOAb and TGAb, and by thyroid gland destruction resulting from a large infiltration of plasma cells and lymphocytes. Factors that enhance the possibility of occurrence of HT mainly include genetic factors,

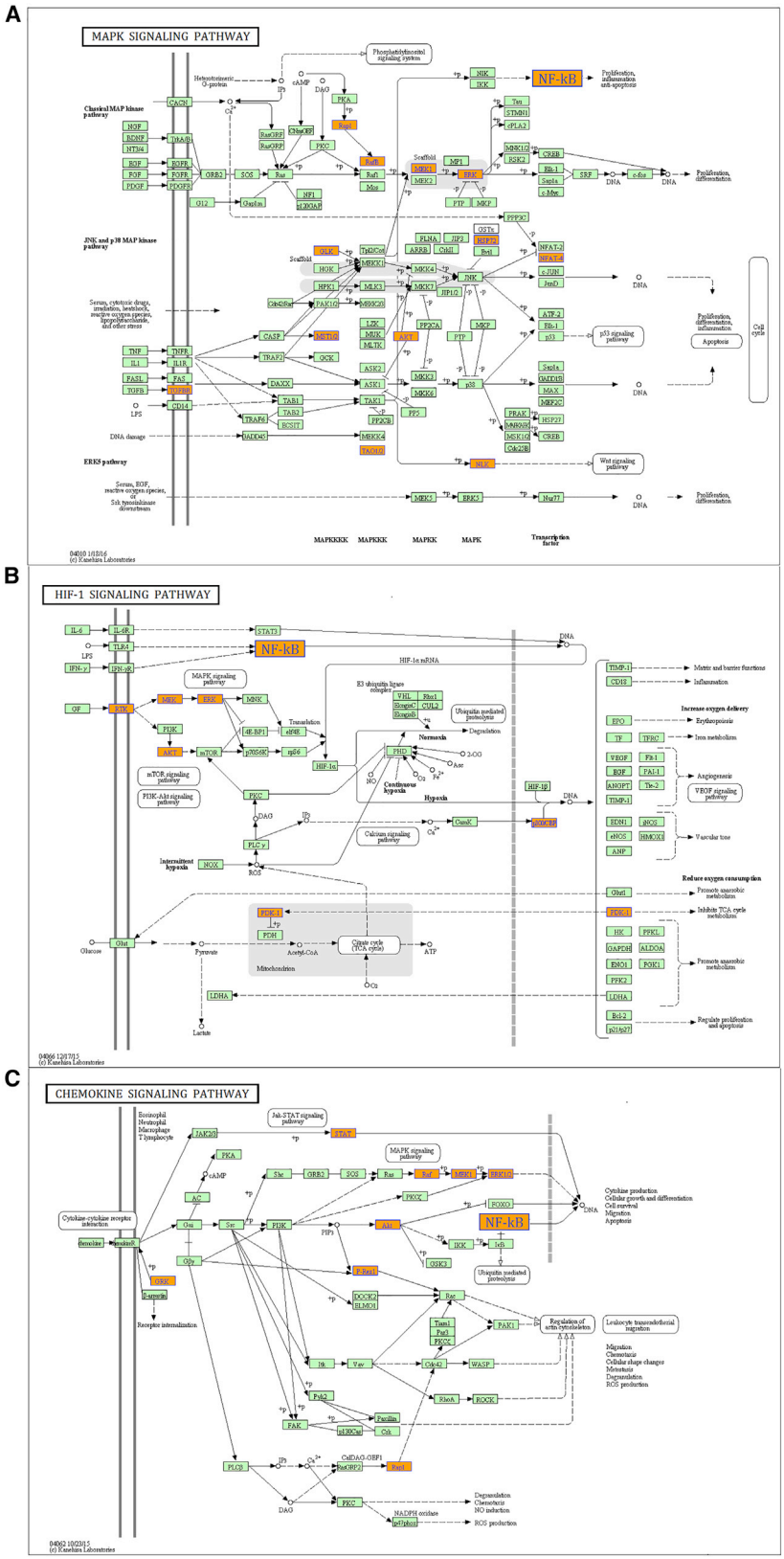

Figure 4. MAPK, HIF-1, and Chemokine Signaling Pathways Regulated by the Upregulated circRNAs in Hashimoto's Thyroiditis

The Kyoto Encyclopedia of Genes and Genomes (KEGG) analysis revealed 73 signaling pathways related to the 370 upregulated circRNAs in patients with HT. (A) Mitogen-activated protein kinases (MAPK), (B) hypoxia inducible factor-1 (HIF-1), and (C) chemokine signaling pathways were connected with expression of NF-kB, which played a crucial role in pathogenesis of HT.

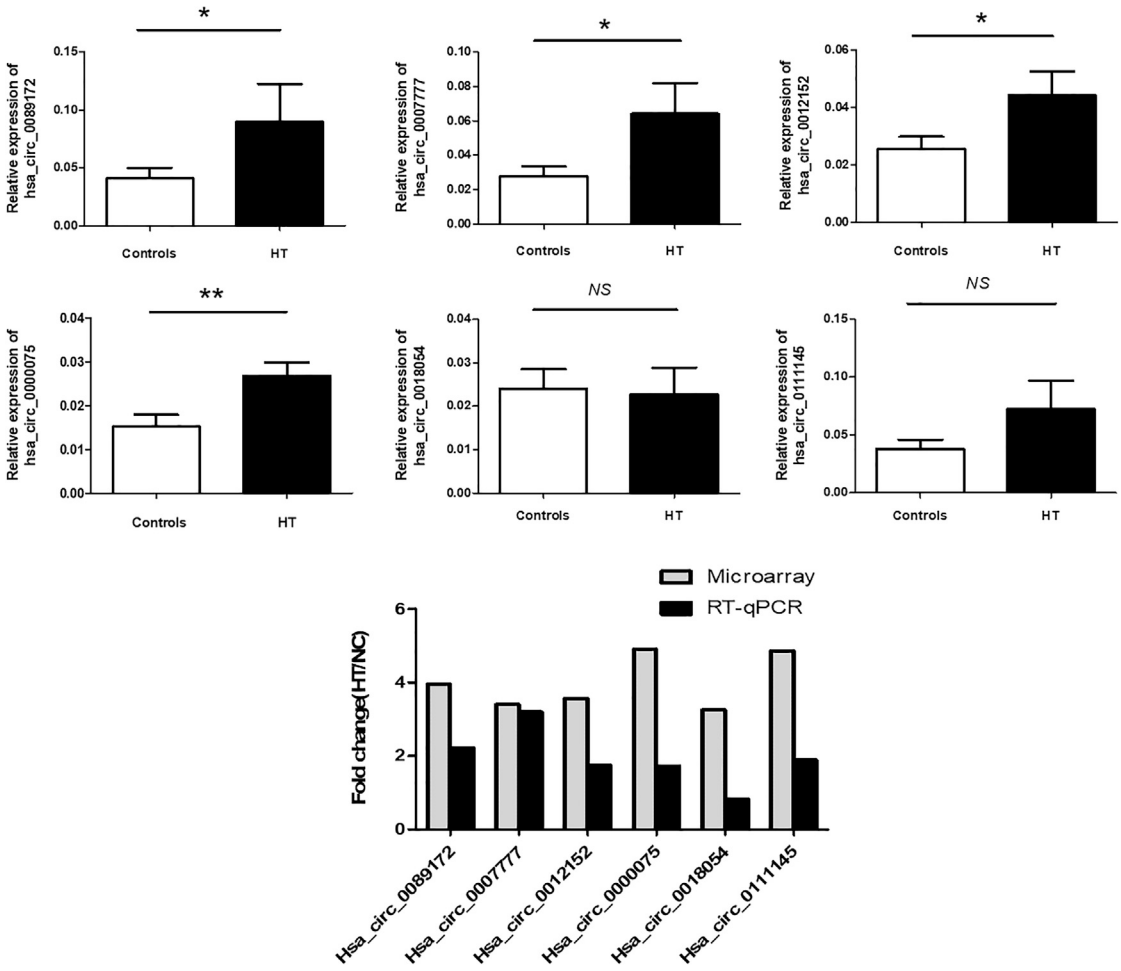

Figure 5. Six Upregulated circRNAs in Patients with Hashimoto's Thyroiditis Compared with Normal Controls

PBMCs from 30 patients with Hashimoto's thyroiditis (HT) and 30 healthy volunteers were used for verification by real-time qPCR on the basis of circRNAs sequencing. The upregulated magnitudes of the six circRNAs were exhibited as fold change in the HT group in relation to the normal control group (NC). The relative expression of the six upregulated circRNAs in PBMCs from HT compared with NC were verified by real-time qPCR. hsa_circ_0089172 ($p = 0.02$), hsa_circ_0007777 ($p = 0.01$), hsa_circ_0012152 ($p = 0.01$), and hsa_circ_0000075 ($p < 0.01$) exhibited the same growing trend toward the sequencing results. Expression of hsa_circ_0018054 and hsa_circ_0111145 showed no statistically significant difference between the HT and NC groups.

immune effects, and environmental influences. Immune mechanisms hold the dominant position.[1,6,7] However, details of the mechanisms remain ambiguous. Therefore, it is necessary to seek out new biomarkers and explore their functions. circRNAs are among the ncRNAs. The closed circular structure formed by covalent bonds enable circRNAs to resist the degradation of RNA exonuclease, which also differentiates circRNAs from traditional linear RNAs.[21,22] In addition, circRNAs have plenty of binding sites to sponge miRNAs. They could competitively bind to the miRNA and then decrease the inhibitory effect of the miRNA on the expression of target genes.[23,24] Many studies have proved that circRNAs are potential biomarkers and participate in pathogenesis of various autoimmune diseases.[25–27] For instance, decreased hsa_circ_0044235 in PBMCs has been confirmed to have significant value in the diagnosis of RA. Risk scores based on hsa_circ_0044235 have distinguished patients with RA from patients with SLE.[28] hsa_circ_0001859 regulates the expression of ATF2 by sponging miR204/211, which promotes inflammation in SW982 cells.[15] However, the functional mechanism of circRNAs in HT is poorly understood. Hence, it would be meaningful to profile circRNA expression and search for new biomarkers, which may contribute to providing new directions and strategies for disease diagnosis and treatment.

Our research identified 627 differentially expressed circRNAs, with 370 upregulated and 257 downregulated, in PBMCs of patients with HT. As far as we know, this is the first description of expression profiling of circRNAs in HT. Our results may enrich the study of the pathogenesis of HT and provide a theoretical basis for the in-depth exploration of the function of circRNAs in HT. We increased the number of samples and carried out real-time qPCR to verify

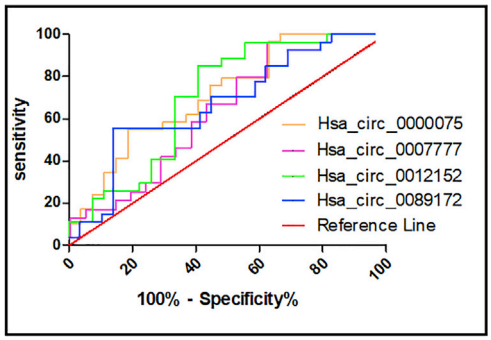

Variables	AUC	P value	SEM	95% C.I.	Sensitivity	Specificity
Has_circ_0089172	0.673	0.026	0.073	0.530-0.816	55.56	86.21
Has_circ_0007777	0.643	0.102	0.085	0.476-0.809	79.17	38.10
Has_circ_0012152	0.702	0.010	0.073	0.559-0.846	85.19	59.26
Has_circ_0000075	0.715	0.006	0.069	0.581-0.849	55.17	81.48

Figure 6. ROC Curve Analysis of Confirmed CircRNAs in PBMCs
The ROC curves of confirmed circRNAs showed that expression of hsa_circ_0089172, hsa_circ_0000075, and hsa_circ_0012152 have potential value in the diagnosis of HT.

sequencing results. We chose six circRNAs from the upregulated ones according to their expression distribution in each specimen. As a consequence, hsa_circ_0089172 ($p = 0.02$), hsa_circ_0007777 ($p = 0.01$), hsa_circ_0012152 ($p = 0.01$), and hsa_circ_0000075 ($p < 0.01$) were verified to be markedly upregulated in the HT group. Then, we conducted ROC curve analysis to further evaluate their diagnostic value.[29] The most valuable one was hsa_circ_0000075 (AUC 0.715, 95% CI 0.581–0.849, $p = 0.006$), followed by hsa_circ_0012152 (AUC 0.702, 95% CI 0.559–0.846, $p = 0.010$) and hsa_circ_0089172 (AUC 0.673, 95% CI 0.530–0.816, $p = 0.026$). Moreover, GO enrichment analysis suggested that circRNAs are involved in a variety of biological processes, such as vitamin D receptor and MAPK binding. In addition, it has been reported that low levels of vitamin D may be involved in the occurrence of HT.[30–32] It has also been suggested that MRP14 takes part in the pathogenetic process of HT through regulating the MAPK signal pathway.[33] These findings reveal a connection between circRNAs and HT. In the meantime, among the 73 pathways relevant to upregulated circRNAs identified by KEGG analysis, the MAPK,[34,35] HIF-1,[36,37] and chemokine[38,39] signaling pathways are related to the expression of NF-κB, which has been shown to be connected with the inflammatory response in HT.[40,41] The results also demonstrated that upregulated circRNAs had great significance in the pathogenesis of HT. As it is well known that circRNAs can function as miRNA sponges, the top 5 miRNAs correlating with the 21 upregulated circRNAs were identified for further study and are shown in the form of a tree diagram. For instance, the five miRNA binding sites of hsa_circ_0089172 were hsa-miR-3620-5p, hsa-miR-6812-5p, hsa-miR-125a-3p, hsa-miR-4463, and hsa-miR-1587.

We are excited to report that we verified that decreased expression of miR-125a-3p may be involved in the pathogenetics of HT through regulating the expression of IL-23R. MiR-125a-3p could modulate IL-23R expression by directly targeting the 3′ UTR of IL-23R mRNA. Moreover, there is a negative correlation between the expression of miR-125a-3p and that of thyroid autoantibodies,[20,42] and IL-23 could interact with its receptor IL-23R on Th17 cells and then facilitate intracellular signaling, which contributes to proliferation and differentiation of Th17 cells.[43] Th17 cells have been demonstrated to play an essential role in the pathogenesis of HT.[44,45] Subsequently, we found that not only did hsa_circ_0089172 match perfectly with miR-125a-3p via specific binding sequences, but expression of the upregulated hsa_circ_0089172 was notably related to that of the downregulated miR-125a-3p. To investigate the role of hsa_circ_0089172 in human PBMCs, we used hsa_circ_0089172-specific siRNA to knock down hsa_circ_0089172 and observed the alteration of miR-125a-3p and IL-23R mRNA. When hsa_circ_0089172 was knocked down with siRNA, the expression of miR-125a-3p increased while the expression of IL-23R mRNA decreased, which provides direct evidence that hsa_circ_0089172 negatively regulates the expression of miR-125a-3p and then influence expression of IL-23R mRNA in PBMCs *in vitro*. However, the epigenetic mechanism of hsa_circ_0089172 that promotes expression of miR-125a-3p in PBMCs is poorly understood. Taken together, the results of our research demonstrate that hsa_circ_0089172 may alter the expression of IL-23R through negatively regulating expression of miR-125a-3p, promoting the occurrence of HT. Therefore, the specific functional mechanism of hsa_0089172 in HT is worthy of further study.

The association between hsa_circ_0089172 and miR-125a-3p may provide a new theoretical basis for research on circRNAs and promote the use of hsa_circ_0089172 as a valuable biomarker in HT. TPOAb and TGAb are important clinical parameters of HT. It has been confirmed that there is a positive connection between the expression of $PD1^+$ T follicular helper (Tfh) cells and TGAb, and Tfh17 cell percentages correlate positively with the expression of TGAb and TPOAb.[46] In this research, a positive correlation was found between expression of hsa_circ_0089172 and TPOAb, whereas the correlation between the expression of hsa_circ_0089172 and TGAb had no statistical significance. The reason for this difference also deserves further exploration. In the future, the function of other differentially expressed circRNAs should be explored in a larger sample. Further cell and animal model experiments should be conducted to increase comprehension of the detailed mechanism and specific functions of circRNAs in HT.

For the first time, to our knowledge, our results provide a profile of circRNA expression and the connection between circRNAs and miRNAs in HT. The relationship between hsa_circ_0089172 and disease severity suggests that hsa_circ_0089172 plays a critical role in the development of HT. Inverse correlation and perfect binding sequences between elevated hsa_circ_0089172 and reduced miR-125a-3p indicate that hsa_circ_0089172 may be involved in

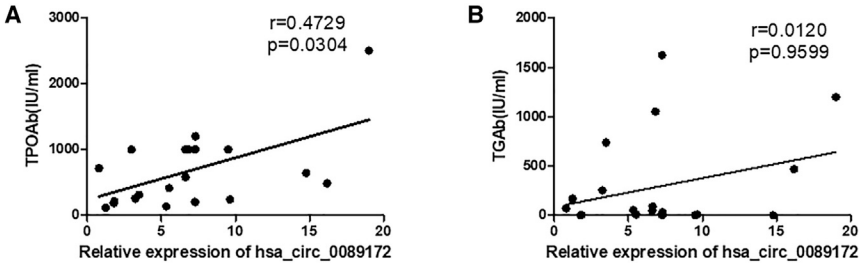

Figure 7. Correlation between hsa_circ_0089172 and Clinical Disease Activities

(A) Expression of hsa_circ-0089172 correlated positively with the expression of TPOAb in plasma. (B) There was no significant association between expression of hsa_circ_0089172 and that of TGAb in patients with HT.

pathogenesis of HT via sponging miR125a-3p. The increase in miR-125a-3p and reduction in IL-23R mRNA resulting from the knockdown of hsa_circ_0089172 demonstrate the regulation by hsa_circ_0089172 of the expression of miR-125a-3p and IL-23R mRNA in PBMCs *in vitro*. In summary, hsa_circ_0089172 is of potentially significant value in HT diagnosis, but there remains a need to further study the mechanisms of hsa_circ_0089172 in HT.

MATERIALS AND METHODS

Collection of Samples

A total of 35 untreated patients with HT and 35 healthy volunteers undergoing physical examinations in the Affiliated People's Hospital of Jiangsu University, who signed the informed-consent form, were enrolled in the research. From that sample, we chose five female patients and five female volunteers for sequencing, because HT is more common in women. The main clinical traits of these participants are summarized in Tables S2 and S3. Clinical symptoms, B-ultrasonography, and laboratory examination were taken as the inclusion criteria. The DxH 800 system (Beckman Coulter, Brea, CA, USA) was used to detect the plasma concentrations of free triiodothyronine (FT3), free thyroxine (FT4), thyroid-stimulating hormone (TSH), TPOAb, and TGAb, according to the manufacturer's instructions. All patients had a positive test for TGAb and TPOAb. Age and gender of the healthy controls matched those of the patients. All NCs were free of thyroid-specific autoantibodies and had no past record of thyroid disease or other autoimmune diseases. Results of routine blood test in the participants were within normal limits. The PBMCs were separated immediately from 10 blood samples and were stored at −80°C until RNA extraction.

Extraction and Quality Control of RNA

Total RNA was extracted from the PBMCs of the 10 samples with Trizol (Life Technologies, Carlsbad, CA, USA). The Nano-Drop ND-1000 instrument (Thermo Fisher Scientific, Waltham, MA, USA) was used to evaluate the concentration of each RNA sample. All RNA samples involved in this research met standards of quality control based on the qualified ratio of OD260 to OD280 (1.8–2.1). RNA integrity and gDNA contamination were measured by modified agarose gel electrophoresis. The quality of the test library was conducted with an Agilent 2100 Bioanalyzer.

Library Preparation of RNA and circRNA Sequencing

Library preparation of RNA and high-throughput sequencing were carried out by Cloud-Seq Biotech (Shanghai, China). According to the supplier's instructions, the Ribozero rRNA Removal Kit (Illumina, San Diego, CA, USA) was applied to remove the rRNAs from total RNA. RNA preprocessing for constructing the sequencing library was implemented with the TruSeq Stranded Total RNA Library Prep Kit (Illumina). Quality control and quantification of the libraries were performed with the Bio-Analyzer 2100 system (Agilent Technologies, Santa Clara, CA, USA). The 10 pM libraries were changed into single-stranded DNA molecules, captured on Illumina Flow Cells, and then amplified *in situ* as clusters, which were subsequently sequenced for 150 cycles on the Illumina Hi-Seq sequencing instrument, using the two-terminal mode (PE mode).

circRNA Profiling Analysis

Paired-end reads were harvested from the Illumina Hi-Seq 4000 sequencer, and the quality score was set at Q30. After 3′ adaptor trimming and removal of poor-quality by Cutadapt software (v1.9.3), the superior quality, trimmed reads were used for analysis of the circRNAs. STAR software (v2.5.1b) was used to make high-quality reads aligned to the reference genome/transcriptome. circRNAs were explored and identified with DCC software (v0.4.4). Identified circRNAs were annotated by the circBase database, and Circ2Traits. EdgeR software (v3.16.5) was applied to filter the differentially expressed circRNA and for data standardization. Significantly differentially expressed circRNAs were the ones that met the standards of fold change $\geq$ 2.0 and p value $\leq$ 0.05. GO and KEGG analysis of differentially expressed circRNA-associated genes were performed to predict functions of these circRNAs. An interactive approach between hsa_circ_0089172 and miR-125a-3p was explored by TargetScan and miRanda. The interaction network between circRNAs and their downstream miRNAs was constructed by Cytoscape software (v2.8.0) based on data of circRNAs with this miRNA binding site and their predicted miRNA sites.

Validation with Real-Time qPCR

PBMCs from 30 patients with HT and 30 healthy controls were used for validation of six upregulated circRNAs by real-time qPCR.[47] Total RNA obtained from PBMCs with Trizol (Invitrogen, Carlsbad, CA USA) was used for synthesizing of cDNAs with the ReverTraAc real-time qPCR kit (Toyobo, Osaka, Japan). First-strand cDNA (2 μL) was used for PCR performed in triplicate, with SYBR Green Super Mix (Bio-Rad, Hercules, CA, USA). Primer sequences are summarized in Table S4. β-Actin was applied as an internal reference for circRNAs to avoid potential aberrance in concentration and efficiency of transcription. Relative expression of circRNAs and IL-23R

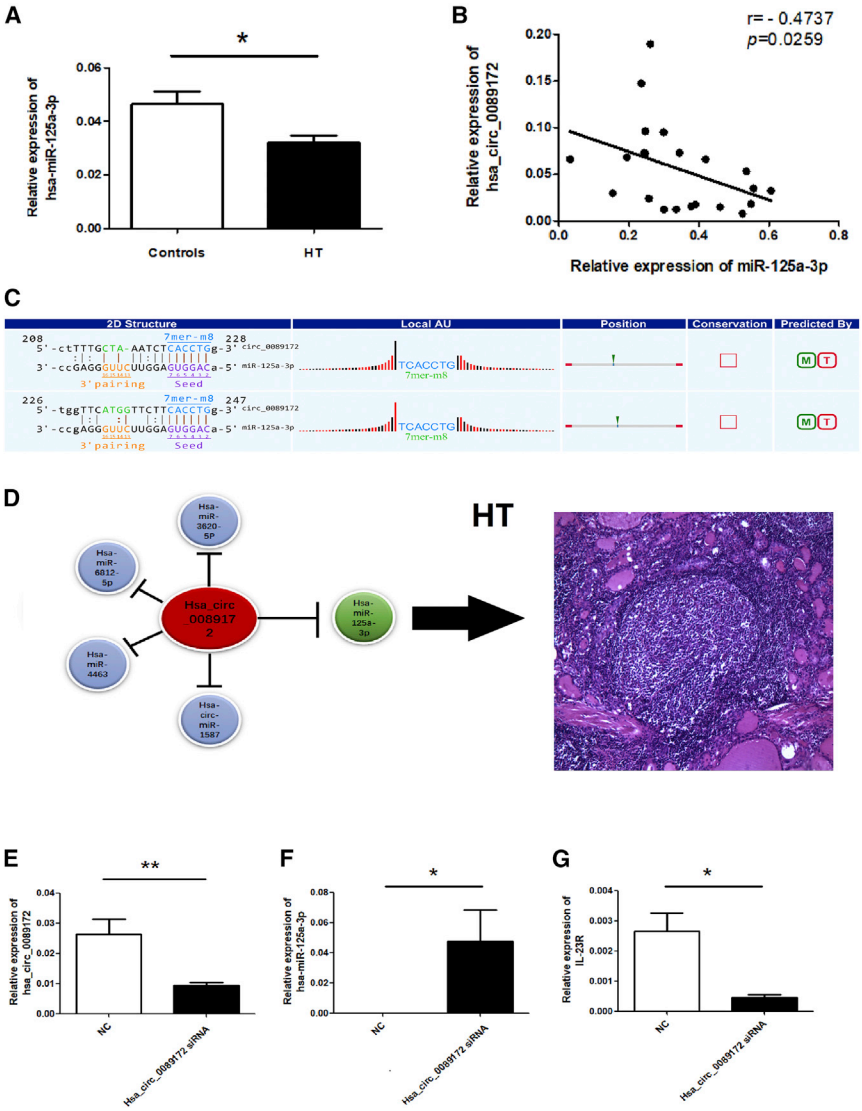

Figure 8. Interaction between hsa_circ_0089172 and hsa-miR-125a-3p in Hashimoto's Thyroiditis

(A) Expression of miR-125a-3p was significantly decreased in patients with Hashimoto's thyroiditis (HT) compared with the NCs, by real-time qPCR. (B) The expression of miR-125-3p showed negative correlation with levels of hsa_circ_0089172 in HT. (C) The interaction between hsa_circ_0089172 and miR-125a-3p was predicted by TargetScan and miRanda. The 2D Structure column showed that there were two perfect binding sequences between hsa_circ_0089172 and miR-125a-3p. The Local AU column displays 30 nucleotides upstream and downstream of the seed sequence. The Position column indicates the probable position of the miR-125a-3p response element on the linear presentation of hsa_circ_0089172. (D) Schematic diagram of mutual relations between hsa_circ_0089172 and miR-125a-3p and other miRNAs indicate the sponge mechanism. A pathological section from a patient with HT is also displayed. (E) The relative expression of hsa_circ_0089172 was determined by real-time qPCR after transfection with siRNA. (F and G) The relative expression of miR-125a-3p (F) and miRNA of IL-23R (G) was determined by real-time qPCR after transfection with siRNA. The results are indicated as the means ± SD of three independent experiments; horizontal lines show the mean (*$p < 0.05$; **$p < 0.01$; ***$p < 0.001$).

were measured by the $2^{-\Delta Ct}$ method for each circRNA. Relative expression of miR-125a-3p was calculated by the same real-time qPCR method as was applied in the verification of circRNAs. U6 was used as an endogenous control gene for miR-125a-3p.

siRNA Knockdown

siRNA (Ribobio, Guangzhou, China) was designed against the sequence of hsa_circ_0089172. Nonspecific scrambled siRNA was used as the NC. The purified PBMCs of healthy volunteers were transfected with hsa_circ_0089172 siRNA or NC at a 100 nM dose, using the Entranster-R (Engreen Biosystem, Beijing, China) in accordance with the manufacturer's instructions, for 24 h in the presence of 2 μg/mL functional anti-human CD3mAb plus 2 μg/mL functional anti-human CD28mAb (Miltenyi Biotec, Bergisch Gladbach, Germany). The relative expression of hsa_circ_0089172, miR-125a-3p, and IL-23R mRNA in PBMCs after being transfected with the hsa_circ_0089172 siRNA or negative control were measured by real-time qPCR.

Statistical Analysis

Student's unpaired t test was used for comparison of two groups. Analysis of difference between the HT group and NC groups was performed with the Mann-Whitney U test. The connection between two variables was decided by Spearman's correlation coefficient. A p value < 0.05 was statistically significant (*$p < 0.05$, **$p < 0.01$, ***$p < 0.001$). GraphPad Prism version 5 software (GraphPad Software, San Diego, CA, USA) was applied for management and analysis of the data.

SUPPLEMENTAL INFORMATION

Supplemental Information can be found online at https://doi.org/10.1016/j.omtn.2019.05.004.

AUTHOR CONTRIBUTIONS

S.X. and H.P. contributed equally to this work, including sample collection, clinical data collection, data analysis, and manuscript writing. Y.L. designed and conducted all the experiments and finalized the manuscript. X.D., X.W., L.W., and C.W. participated in sample and data collection. S.W. and H.X. participated in the design of the experiments. All authors discussed the results and commented on the manuscript.

CONFLICTS OF INTEREST

The authors declare no competing interests.

ACKNOWLEDGMENTS

This work was supported by the National Natural Science Foundation of China (Grant No. 81800698), the Jiangsu Provincial Key Medical Talents Project (Grant No. QNRC2016455), the Jiangsu Province Fifth Phase "333" Project Training Fund Support (BRA2018184), and the Zhenjiang Science and Technology Planning Project (Grant No. SH2016043, SH2018051).

REFERENCES

1. Rydzewska, M., Jaromin, M., Pasierowska, I.E., Stożek, K., and Bossowski, A. (2018). Role of the T and B lymphocytes in pathogenesis of autoimmune thyroid diseases. Thyroid Res. *11*, 2.
2. Caturegli, P., De Remigis, A., Chuang, K., Dembele, M., Iwama, A., and Iwama, S. (2013). Hashimoto's thyroiditis: celebrating the centennial through the lens of the Johns Hopkins hospital surgical pathology records. Thyroid *23*, 142–150.
3. Voisin, G., Delaunay, A., and Barber, M. (1951). [Testicular lesions induced in the guinea pig by iso- and auto-sensitization]. Ann. Inst. Pasteur (Paris) *81*, 48–63.
4. Wufuer, Y., Wang, H., Halimulati, and Xinxi, L. (2018). The differential diagnostic value of TSH and TPOAb levels in Hashimoto's thyroiditis and papillary thyroid carcinoma. Chinese Journal of Difficult and Complicated Cases *2018*, 387–390.
5. Štefanić, M., Tokić, S., Suver Stević, M., and Glavaš-Obrovac, L. (2018). Association of increased eomesodermin, BCL6, and granzyme B expression with major clinical manifestations of Hashimoto's thyroiditis - an observational study. Immunol. Invest. *47*, 279–292.
6. Guo, Y., Zynat, J., Xing, S., Xin, L., Li, S., Mammat, N., Chen, Y., Zhao, L., Zhao, H., and Wang, X. (2018). Immunological changes of T helper cells in flow cytometer-sorted $CD4^+$ T cells from patients with Hashimoto's thyroiditis. Exp. Ther. Med. *15*, 3596–3602.
7. Hu, S., and Rayman, M.P. (2017). Multiple Nutritional Factors and the Risk of Hashimoto's Thyroiditis. Thyroid *27*, 597–610.
8. Barić, A., Brčić, L., Gračan, S., Torlak Lovrić, V., Gunjača, I., Šimunac, M., Brekalo, M., Boban, M., Polašek, O., Barbalić, M., et al. (2017). Association of established hypothyroidism-associated genetic variants with Hashimoto's thyroiditis. J. Endocrinol. Invest. *40*, 1061–1067.
9. Kowalczyk, A., Zegan, M., and Michota-Katulska, E. (2017). [Key minerals significant for hypothyroidism including Hashimoto's thyroiditis - function and presence in food]. Wiad. Lek. *70*, 778–783.
10. Ling, H. (2016). Non-coding RNAs: Therapeutic Strategies and Delivery Systems. Adv. Exp. Med. Biol. *937*, 229–237.
11. Matsui, M., and Corey, D.R. (2017). Non-coding RNAs as drug targets. Nat. Rev. Drug Discov. *16*, 167–179.
12. Metge, F., Czaja-Hasse, L.F., Reinhardt, R., and Dieterich, C. (2017). FUCHS-towards full circular RNA characterization using RNAseq. PeerJ *5*, e2934.
13. Vicens, Q., and Westhof, E. (2014). Biogenesis of Circular RNAs. Cell *159*, 13–14.
14. Zhong, Y., Du, Y., Yang, X., Mo, Y., Fan, C., Xiong, F., Ren, D., Ye, X., Li, C., Wang, Y., et al. (2018). Circular RNAs function as ceRNAs to regulate and control human cancer progression. Mol. Cancer *17*, 79.
15. Li, B., Li, N., Zhang, L., Li, K., Xie, Y., Xue, M., and Zheng, Z. (2018). Hsa_circ_0001859 Regulates ATF2 Expression by Functioning as an MiR-204/211 Sponge in Human Rheumatoid Arthritis. J. Immunol. Res. *2018*, 9412387.
16. Hall, I.F., Climent-Salarich, M., Quintavalle, M., Farina, F.M., Schorn, T., Zani, S.M., Carullo, P., Kunderfranco, P., Civilini, E., Condorelli, G., and Elia, L. (2019). Circ_Lrp6, a Circular RNA Enriched in Vascular Smooth Muscle Cells, Acts as a Sponge Regulating miRNA-145 Function. Circ. Res. *124*, 498–510.
17. Yang, F., Fang, E., Mei, H., Chen, Y., Li, H., Li, D., Song, H., Wang, J., Hong, M., Xiao, W., et al. (2019). *Cis*-acting circ-CTNNB1 promotes beta-catenin signaling and cancer progression via DDX3-mediated transactivation of YY1. Cancer Res. *79*, 557–571.
18. Li, L.J., Zhu, Z.W., Zhao, W., Tao, S.S., Li, B.Z., Xu, S.Z., Wang, J.B., Zhang, M.Y., Wu, J., Leng, R.X., et al. (2018). Circular RNA expression profile and potential function of hsa_circ_0045272 in systemic lupus erythematosus. Immunology *155*, 137–149.
19. Ouyang, Q., Wu, J., Jiang, Z., Zhao, J., Wang, R., Lou, A., Zhu, D., Shi, G.P., and Yang, M. (2017). Microarray Expression Profile of Circular RNAs in Peripheral Blood Mononuclear Cells from Rheumatoid Arthritis Patients. Cell. Physiol. Biochem. *42*, 651–659.
20. Peng, H., Liu, Y., Tian, J., Ma, J., Tang, X., Yang, J., Rui, K., Zhang, Y., Mao, C., Lu, L., et al. (2015). Decreased expression of microRNA-125a-3p upregulates interleukin-23 receptor in patients with Hashimoto's thyroiditis. Immunol. Res. *62*, 129–136.
21. Ebbesen, K.K., Hansen, T.B., and Kjems, J. (2017). Insights into circular RNA biology. RNA Biol. *14*, 1035–1045.
22. Kulcheski, F.R., Christoff, A.P., and Margis, R. (2016). Circular RNAs are miRNA sponges and can be used as a new class of biomarker. J. Biotechnol. *238*, 42–51.
23. Kun-Peng, Z., Chun-Lin, Z., Jian-Ping, H., and Lei, Z. (2018). A novel circulating hsa_circ_0081001 act as a potential biomarker for diagnosis and prognosis of osteosarcoma. Int. J. Biol. Sci. *14*, 1513–1520.
24. Ashwal-Fluss, R., Meyer, M., Pamudurti, N.R., Ivanov, A., Bartok, O., Hanan, M., Evantal, N., Memczak, S., Rajewsky, N., and Kadener, S. (2014). circRNA biogenesis competes with pre-mRNA splicing. Mol. Cell *56*, 55–66.
25. Zhang, M.Y., Wang, J.B., Zhu, Z.W., Li, L.J., Liu, R.S., Yang, X.K., Leng, R.X., Li, X.M., Pan, H.F., and Ye, D.Q. (2018). Differentially expressed circular RNAs in systemic lupus erythematosus and their clinical significance. Biomed. Pharmacother *107*, 1720–1727.
26. Wang, X., Zhang, C., Wu, Z., Chen, Y., and Shi, W. (2018). CircIBTK inhibits DNA demethylation and activation of AKT signaling pathway via miR-29b in peripheral blood mononuclear cells in systemic lupus erythematosus. Arthritis Res. Ther *20*, 118.
27. Tian, Y., Xu, Y., Wang, H., Shu, R., Sun, L., Zeng, Y., Gong, F., Lei, Y., Wang, K., and Luo, H. (2019). Comprehensive analysis of microarray expression profiles of circRNAs and lncRNAs with associated co-expression networks in human colorectal cancer. Funct. Integr. Genomics *19*, 311–327.
28. Luo, Q., Zhang, L., Li, X., Fu, B., Deng, Z., Qing, C., Su, R., Xu, J., Guo, Y., Huang, Z., and Li, J. (2018). Identification of circular RNAs hsa_circ_0044235 in peripheral blood as novel biomarkers for rheumatoid arthritis. Clin. Exp. Immunol. *194*, 118–124.
29. Kamarudin, A.N., Cox, T., and Kolamunnage-Dona, R. (2017). Time-dependent ROC curve analysis in medical research: current methods and applications. BMC Med. Res. Methodol *17*, 53.
30. Kim, D. (2016). Low vitamin D status is associated with hypothyroid Hashimoto's thyroiditis. Hormones (Athens) *15*, 385–393.
31. Xu, J., Zhu, X.Y., Sun, H., Xu, X.Q., Xu, S.A., Suo, Y., Cao, L.J., Zhou, Q., Yu, H.J., and Cao, W.Z. (2018). Low vitamin D levels are associated with cognitive impairment in patients with Hashimoto thyroiditis. BMC Endocr. Disord. *18*, 87.
32. Krysiak, R., Szkróbka, W., and Okopień, B. (2017). The Effect of Vitamin D on Thyroid Autoimmunity in Levothyroxine-Treated Women with Hashimoto's Thyroiditis and Normal Vitamin D Status. Exp. Clin. Endocrinol. Diabetes *125*, 229–233.
33. Luo, X., Zheng, T., Mao, C., Dong, X., Mou, X., Xu, C., Lu, Q., Liu, B., Wang, S., and Xiao, Y. (2018). Aberrant MRP14 expression in thyroid follicular cells mediates

chemokine secretion through the IL-1β/MAPK pathway in Hashimoto's thyroiditis. Endocr. Connect *7*, 850–858.

34. Lopez, S., Gomez, E., Torres, M.J., Pozo, D., Fernandez, T.D., Ariza, A., Sanz, M.L., Blanca, M., and Mayorga, C. (2015). Betalactam antibiotics affect human dendritic cells maturation through MAPK/NF-kB systems. Role in allergic reactions to drugs. Toxicol. Appl. Pharmacol *288*, 289–299.

35. Kang, H.H., Kim, I.K., Lee, H.I., Joo, H., Lim, J.U., Lee, J., Lee, S.H., and Moon, H.S. (2017). Chronic intermittent hypoxia induces liver fibrosis in mice with diet-induced obesity via TLR4/MyD88/MAPK/NF-kB signaling pathways. Biochem. Biophys. Res. Commun. *490*, 349–355.

36. Deng, W., Feng, X., Li, X., Wang, D., and Sun, L. (2016). Hypoxia-inducible factor 1 in autoimmune diseases. Cell. Immunol *303*, 7–15.

37. Wu, S.L., Li, Y.J., Liao, K., Shi, L., Zhang, N., Liu, S., Hu, Y.Y., Li, S.L., and Wang, Y. (2017). 2-Methoxyestradiol inhibits the proliferation and migration and reduces the radioresistance of nasopharyngeal carcinoma CNE-2 stem cells via NF-κB/HIF-1 signaling pathway inactivation and EMT reversal. Oncol. Rep. *37*, 793–802.

38. Sowa, J.E., Ślusarczyk, J., Trojan, E., Chamera, K., Leśkiewicz, M., Regulska, M., Kotarska, K., and Basta-Kaim, A. (2017). Prenatal stress affects viability, activation, and chemokine signaling in astroglial cultures. J. Neuroimmunol *311*, 79–87.

39. Gallagher, S.J., Mijatov, B., Gunatilake, D., Gowrishankar, K., Tiffen, J., James, W., Jin, L., Pupo, G., Cullinane, C., McArthur, G., et al. (2014). Control of NF-kB activity in human melanoma by bromodomain and extra-terminal protein inhibitor I-BET151. Pigment Cell Melanoma Research *27*, 1126–1137.

40. Koc, A., Batar, B., Celik, O., Onaran, I., Tasan, E., and Sultuybek, G.K. (2014). Polymorphism of the NFKB1 affects the serum inflammatory levels of IL-6 in Hashimoto thyroiditis in a Turkish population. Immunobiology *219*, 531–536.

41. Mörs, K., Hörauf, J.A., Kany, S., Wagner, N., Sturm, R., Woschek, M., Perl, M., Marzi, I., and Relja, B. (2017). Ethanol Decreases Inflammatory Response in Human Lung Epithelial Cells by Inhibiting the Canonical NF-kB-Pathway. Cell Physiol. Biochem *43*, 17–30.

42. Li, Z.H., Han, J., Wang, Y.F., Dai, J., Zhang, H., Li, C.X., and Ma, Q. (2015). Association between Polymorphism of Interleukin-23 Receptor and Hashimoto's Thyroiditis in Chinese Han Population of Shandong. Chin. Med. J. *128*, 2050–2053.

43. Sano, T., Huang, W., Hall, J.A., Yang, Y., Chen, A., Gavzy, S.J., Lee, J.Y., Ziel, J.W., Miraldi, E.R., Domingos, A.I., et al. (2015). An IL-23R/IL-22 Circuit Regulates Epithelial Serum Amyloid A to Promote Local Effector Th17 Responses. Cell *163*, 381–393.

44. Li, D., Cai, W., Gu, R., Zhang, Y., Zhang, H., Tang, K., Xu, P., Katirai, F., Shi, W., Wang, L., et al. (2013). Th17 cell plays a role in the pathogenesis of Hashimoto's thyroiditis in patients. Clin. Immunol. *149*, 411–420.

45. Liu, Y., Tang, X., Tian, J., Zhu, C., Peng, H., Rui, K., Wang, Y., Mao, C., Ma, J., Lu, L., et al. (2014). Th17/Treg cells imbalance and GITRL profile in patients with Hashimoto's thyroiditis. Int. J. Mol. Sci. *15*, 21674–21686.

46. Zhao, J., Chen, Y., Zhao, Q., Shi, J., Yang, W., Zhu, Z., Yu, W., Guan, J., Song, Y., Wu, H., et al. (2018). Increased circulating Tfh17 and PD-1^{+}Tfh cells are associated with autoantibodies in Hashimoto's thyroiditis. Autoimmunity *51*, 352–359.

47. Tian, J., Rui, K., Hong, Y., Wang, X., Xiao, F., Lin, X., Ma, J., Guo, H., Xu, H., Ma, K., et al. (2019). Increased GITRL impairs the function of myeloid-derived suppressor cells and exacerbates primary Sjögren's syndrome. J Immunol *202*, 1693–1703.